ORIGINAL PAPER

Physical model experiments for shallow failure in rainfall-triggered loess slope, Northwest China

Ping Sun[1,2] · Gang Wang[1,2] · L. Z. Wu[3] · Ogbonnaya Igwe[4] · Enzhen Zhu[1,2]

Abstract

In order to effectively reduce the impact of rainfall-induced landslides on properties and life, it is important to understand rainfall-caused landslides and their sliding mechanisms. The objective of this paper is to study the effects of different rainfall patterns and different slope structures on the deformation and failure process of shallow loess slopes. To achieve the objective, three categories of indoor physical model experiments of a loess slope with and without a vertical joint were implemented under different rainfall patterns. Three kinds of sensors, including volumetric water content, matric suction, and pore-water pressure sensors, were buried in the model slopes to record the internal changes driving deformation. Analyses of the sensor records and the associated deformational changes, and the experimental results under different conditions show that the matric suction in loess slopes decreased gradually. Loess strength reduced with the continuous increase of volumetric water content. After excess pore-water pressure was generated by the slope deformation and poor drainage of the loess, it decreased the effective stress and the loess strength, which resulted in landslides. In addition, it was observed that the influence of slope structure on stability was greater than that of rainfall patterns. This paper attempts to explain the failure mode and triggering mechanisms of shallow loess landslides induced by rainfall.

Keywords Loess slope · Rainfall-induced landslide · Physical model experiment · Pore-water pressure

Introduction

Based on the literature statistics, about 70% of landslides are caused by rainfall, and up to 95% of the landslides occur in the rainy season. These rainfall-induced landslides not only cause considerable financial losses but also ecological and environmental problems, such as increased soil erosion rate and downstream sediment load (Anderson and Sitar 1995; Hovius et al. 1997; Claessens et al. 2007; Peng et al. 2015, 2017; Wu et al. 2018a). Therefore, studies on rainfall-induced landslides have become an important research topic in recent decades, which have led to the reporting of many rainfall-induced catastrophes worldwide (Crozier 1999; Tsaparas et al. 2002; Chen and Lee 2003; Collins and Znidarcic 2004; Godt et al. 2006; Chang and Chiang 2009; Evans et al. 2009; Tsai 2011; Xu et al. 2011, 2012; Ali et al. 2014; Wang et al. 2014).

Loess is widely distributed in northwest China, covering approximately 631,000 km² , which is about 6.6% of the total land area (Liu 1985), and it is a special type of geological material that is replete with randomly distributed defects of different orders, such as micro fissures, pores, and assorted joints. Its unique structure, the associated vertical joints

✉ L. Z. Wu
  wulizhou07@cdut.cn

  Ping Sun
  sunpingcgs@163.com

  Gang Wang
  1245651731@qq.com

  Ogbonnaya Igwe
  igwejames@hotmail.com

  Enzhen Zhu
  1433716481@qq.com

1 Institute of Geomechanics, Chinese Academy of Geological Sciences, Beijing 100081, China

2 Key Laboratory of Neotectonic Movement and Geohazard, Ministry of Land and Resources, Beijing 100081, China

3 State Key Laboratory of Geohazard Prevention and Geoenvironment Protection, Chengdu University of Technology, Chengdu 610059, Sichuan, China

4 Department of Geology, University of Nigeria, Nsukka, Nigeria

developed inside, and its water sensitivity ensures rapid infiltration of water and increased vulnerability of loess slopes to shallow failures (Gao 1988). Therefore, water is the most active factor for triggering shallow loess landslide. Aleotti (2004) proposed the concept of rainfall thresholds, which represent a simplification of the relationship between rainfall and landslide occurrence. Zhang et al. (2000) thoroughly describe the infiltration process within a weathered jointed granite profile for slope engineering design, a model based on the assumption of a uniform porous media and discontinuities. Based on the variation of volumetric water content and matric suction in soil, a method to analyze the rainfall infiltration is proposed. By means of the gravity-predominant flow (GPF) concept, the infiltration rate is analyzed in the deep soil. The results explain well the observations that loess slopes could be stable in the wet season, but it may tend to slide about 3–6 months later in the dry season. The surface infiltration has a very limited effect on the permanent groundwater table, which is at a greater depth (Guzzetti et al. 2004; Tu et al. 2009).

It can be seen that the field experiment involving artificial rainfall has already been conducted on a loess plateau. Laboratory experiments allow us to analyze soil deformation in a much shorter time, and the forces and dimensions can be chosen based on suitable scaling methods (Rosenau et al. 2009). Furthermore, the materials used in the experiments are made of similar materials, and the slopes are mostly homogenous (Wu et al. 2017, 2018b).

Therefore, in order to more objectively examine the landslide formation mechanism, the quaternary loess material with vertical joint was used and different rainfall forms were considered in the physical model experiments. The purpose of this paper is to study the effects of rainfall patterns and slope structures on the deformation and failure process of shallow loess slope. Shallow loess landslides located at the south Jingyang Plateau, China, were chosen for the study. Three categories of indoor physical model experiments were designed and implemented. The categories include loess slope with continuous heavy rainfall, loess slope containing a vertical joint with continuous heavy rainfall, and loess slope with intermittent heavy rainfall, respectively.

Methods

Three groups of physical model experiments were conducted in Chengdu University of Technology, China. The length × width × height of the model box used in experiments is 1.2 m × 0.4 m × 0.6 m, and the volume is 0.288 m^3. The layout of experiments is shown in Fig. 1.

Experimental soil sample

The loess sample used in experiments was collected from the south Jingyang Plateau, China, with a large amount of shallow loess landslides here (Fig. 2). For the indoor physical model experiments, loess sample was crushed by a hammer and passed through a 5 mm screen. The physical parameters of the loess are shown in Table 1. The distribution curve of the loess is shown in Fig. 3, and the soil water retention curve can be seen in Fig. 4.

Experiment instruments

The experimental instruments mainly consist of seven parts (Fig. 5), including the model box, the artificial rainfall system, the pore-water pressure sensors, the
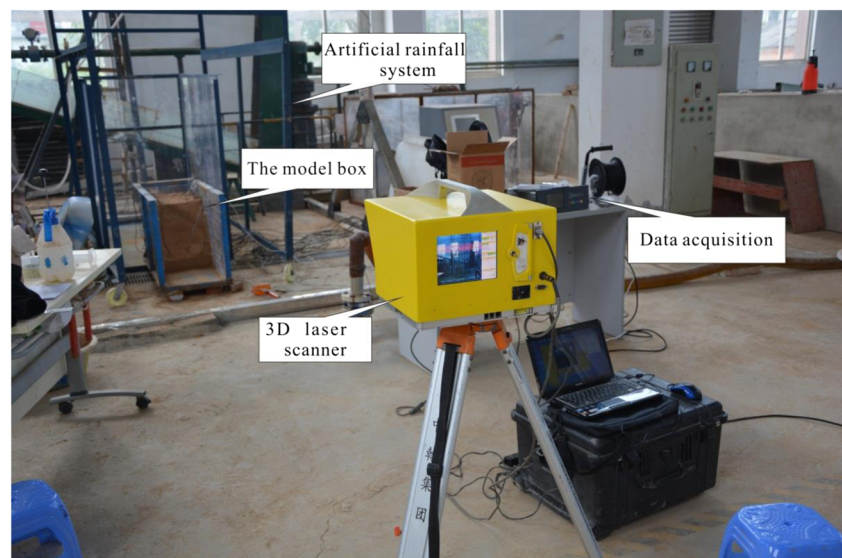

Fig. 1 The layout of experiments

Fig. 2 A typical loess landslide at Jingyang, China

volumetric moisture sensors, the matric suction sensors, the data acquisition instruments, and the 3D laser scanner. In order to observe the deformation and failure process of the slope under rainfall condition, a transparent toughened glass was used in the model box. The artificial rainfall system is mainly composed of rainfall sprayers and a pressure gauge. Aiming to reduce the effect of raindrop erosion on slope, the atomizing nozzle was used, and the distance between two nozzles is 30 cm. The physical model experiments consist of several hydrologic sensors and data acquisition devices that include EC-5 volumetric moisture sensors designed by Decagon with an accuracy of ±2%, the MPS-6 matric suction sensors designed by Decagon with an accuracy of ±10 kPa, the HC-25 pore-water pressure sensors designed by Haichen Tianyu with an accuracy of ±0.1%, EM50 data acquisition designed by Decagon, and pore-water data acquisition instruments designed by Haichen Tianyu (Beijing, China). All the sensors were connected with corresponding data acquisition instruments and were calibrated before experiments. The deformation monitoring instrument used in the experiments was an Optech ILRIS-3D 3D laser scanner produced by the Teledyne Company of Canada, which has a high density scanning ability.

Experimental scheme

The main purpose of these physical model experiments is to study the deformation and failure characteristics of loess slopes during heavy rainfall. The authors designed and conducted three groups of indoor physical model experiments, including loess slope with continuous heavy rainfall, loess slope containing a vertical joint with continuous heavy rainfall, and loess slope with intermittent heavy rainfall, so as to analyze the influence of slope structure and rainfall pattern on loess slopes. In addition, the gradients of three loess slope models are all 60 degrees. During the experimental period, experimenters should record the time from the beginning with a rainfall intensity of 70 mm/h till complete slope failure occurs, and more details about the experimental scheme are shown in Table 2. To ensure the homogeneity of the loess slope, the loess was filled with a lift thickness of 5 cm. Each filling was completed at initial water content. For the loess slope with vertical joint, the positons of the vertical joint were pre-set during filling the slope model, and the crack will be fully filled with quartz sands.
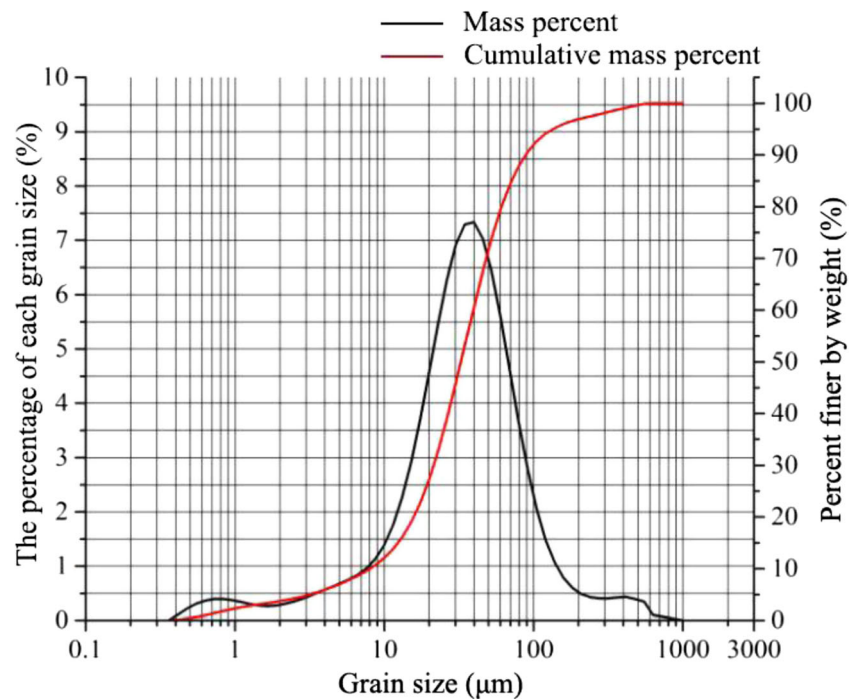
Experimental section of loess slope with continuous and intermittent heavy rainfall

For continuous and intermittent heavy rainfall experiments of the loess slope, the location of sensors buried in the slope and size of the slope are shown in Fig. 6.

Experiments of slope containing a vertical joint with heavy rainfall

Based on a large number of field investigations, the authors have found that the vertical joint in loess is one of the

Table 1 Physical parameters of the loess sample

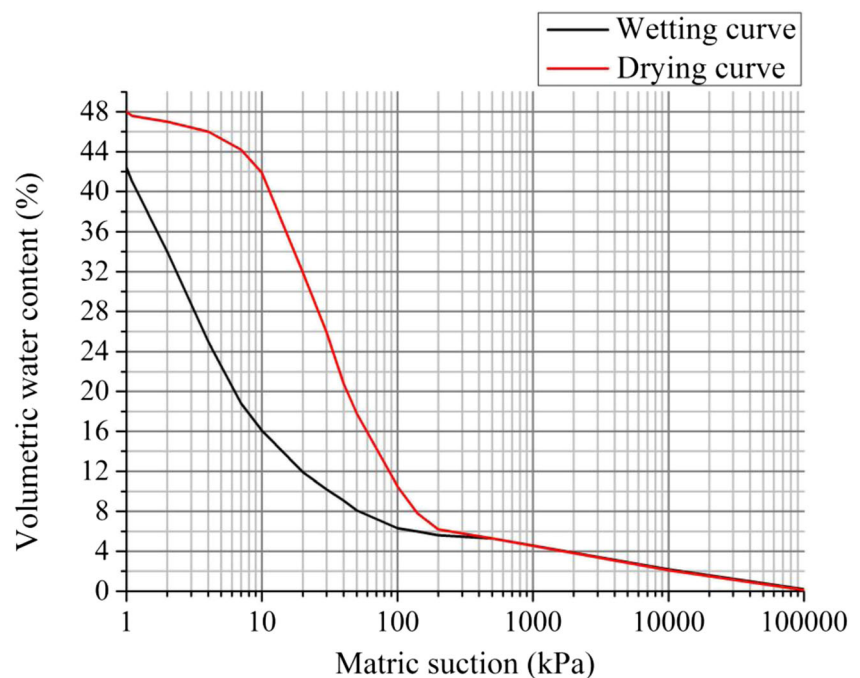| Natural unit weight (kN/m³)	Initial volumetric water content (%)	Saturated volumetric water content (%)	Plastic limit (PL%)	Liquid limit (LL %)	Plasticity index (PI)
14.7	10	43	17.2	28	10.9

Fig. 3 Particle distribution curve
of the loess

important factors affecting slope stability. To reveal the influence of vertical joints on the deformation and failure of slopes, the joint with a size of 0.3 m × 0.2 m × 0.02 m was designed, and the distance between the vertical joint and the shoulder was 20 cm after reducing the size of field loess slope and simplifying the model slope in equal proportion (Fig. 7a). During the field investigation, it was found that the joints in

the trailing edge of the slope were filled with gravels and debris, as a result, the vertical joint in model slope was full of quartz sands. The model slope is shown in Fig. 7b, and Fig. 8 shows the experimental section of the slope.

The experimental study on slope with intermittent heavy rainfall is the same as that of loess slope with continuous heavy rainfall.

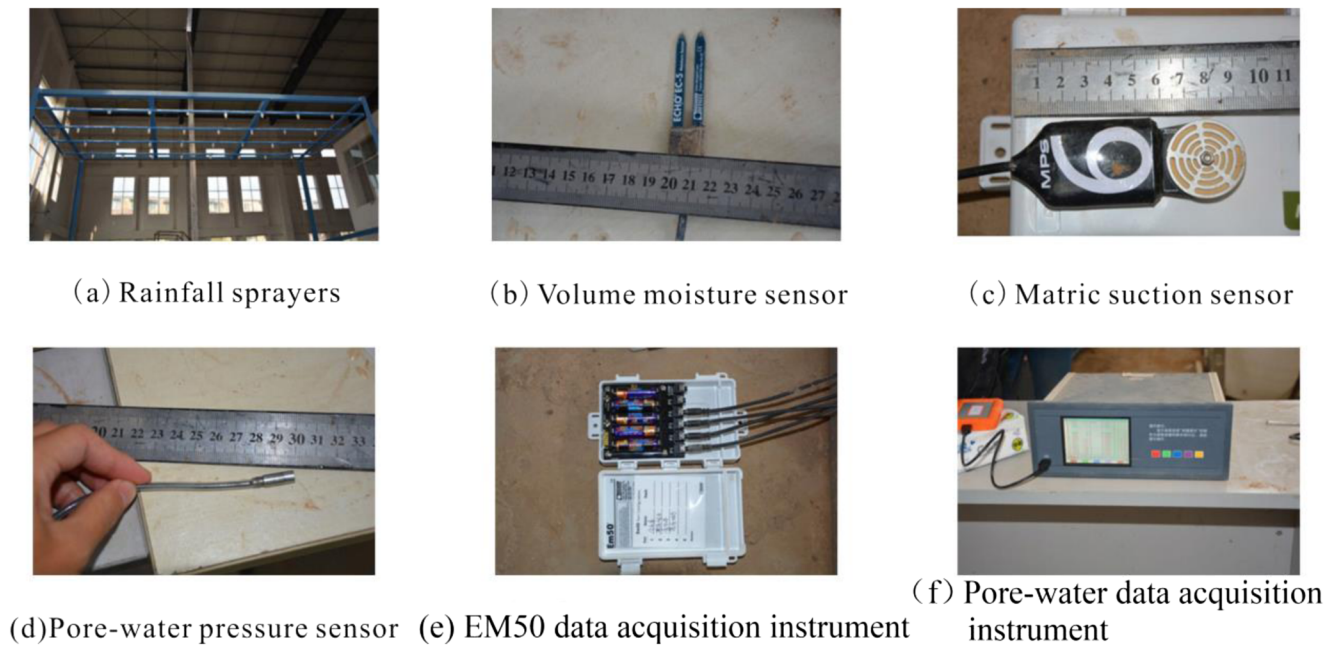**Fig. 4** Soil water retention curve

(a) Rainfall sprayers (b) Volume moisture sensor (c) Matric suction sensor

(d) Pore-water pressure sensor (e) EM50 data acquisition instrument (f) Pore-water data acquisition instrument

Fig. 5 Instruments used in experiments

Analysis on experimental process and results

Experiments would not start until the readings of sensors were stable and then the authors carried out the experiment according to the scheme.

Loess slope with continuous heavy rainfall

Figure 9 shows the process of deformation and failure of loess slope with continuous heavy rainfall. From the changing sensor readings (Figs. 10, 11, and 12), the sequence of seepage velocity from large to small was: toe of slope, trailing edge of the slope and middle slope, under the condition of heavy rainfall. Among the volumetric moisture sensors 2, 5, 6, and 7 buried at 10 cm depths, readings of sensor 7 buried at the foot of the slope rose rapidly at the beginning, and then increased gently for a period until it was stable. Notably, there was no obvious change in the readings when landslide failure occurred.

Readings of sensor 6 located at the trailing edge of the slope changed slightly earlier than that of sensor 5 buried at the shoulder of the slope, while readings of sensor 5 rose slightly when the slope failure happened. Readings of sensor 2 buried at the middle slope changed last, and increased obviously when sliding failure was formed. Among the sensors 1, 3, and 4 buried at 20 cm depths, readings of sensor 1 located at the middle slope initially changed but remained almost unchanged when the slope failure occurred. Then readings of sensor 3 buried under the shoulder of slope increased and showed no obvious change when sliding occurred. The readings of sensor 4 located at the trailing edge of the slope finally started to increase, and the trend of change was the same as that of sensor 3. The order of the decreasing readings of matric suction sensors was in accordance with that of the volumetric moisture sensors, and the difference occurred when the readings of matric suction sensors reached a certain value. The readings remained stable after that. The trend

Table 2 Scheme of rainfall experiments and sliding time

| Experimental types	Rainfall intensity (mm/h)	Precipitation time	Rainfall patterns	Slope types
Loess slope with continuous heavy rainfall experiment	70	Do not stop until the slope failure happens	Continuous heavy rainfall	Homogeneous slope
Loess slope containing a vertical joint with continuous heavy rainfall experiment	70	Do not stop until the slope failure happens	Continuous heavy rainfall	Slope containing a vertical joint
Loess slope with intermittent heavy rainfall experiment	70	Rain for 1 h in every 24 h, until the landslide occurs	Intermittent heavy rainfall	Homogeneous slope
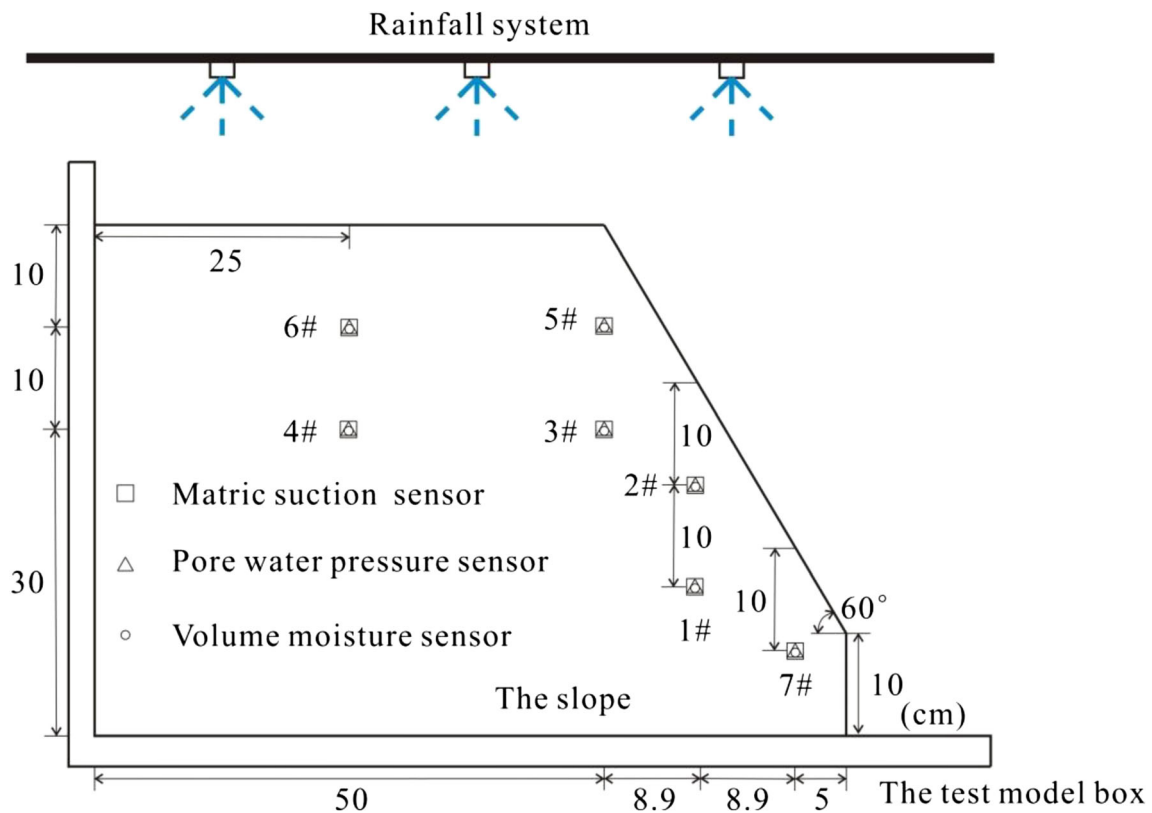
Fig. 6 Experimental section of loess slope with continuous heavy rainfall

of the increasing readings of pore-water pressure sensors coincided with the trend of that of the volumetric water content sensors. During the sliding of the slope, when volumetric water content rose sharply, it was accompanied by a sudden increase in pore-water pressure. It is noted that the greatest increase in the range of readings among all pore-water pressure sensors occurred in sensor 2 located 10 cm below the middle slope.

As for the moisture content sensors (Fig. 10a), sensor 5 is located below the slope shoulder, the rainwater on the trailing edge flows through the shoulder, causing erosion. The No. 2 sensor is located below the slope, and the water is easy to runoff. Compared with sensor 2, the water

content of sensor 5 began to increase earlier. After 2 h and 21 min, the soil becomes basically saturated, and then the water content remained basically unchanged. After 5 h and 20 min, moisture content of sensors 2 and 5 suddenly increased. At this time, the slope slid, then rainfall stops, and the water content decreases slowly. Reading of sensor 2 increases largest among the sensor groups because it was close to the front edge of slip surface when the slope slid.

As for the pore-water pressure sensor, due to the rainwater infiltration, the sensors 5 and 2 began to increase at 17 min and 47 min respectively, and stabilized at 1.6 kPa (1 h, 47 min) and 1.5 kPa (2 h and 20 min) respectively.

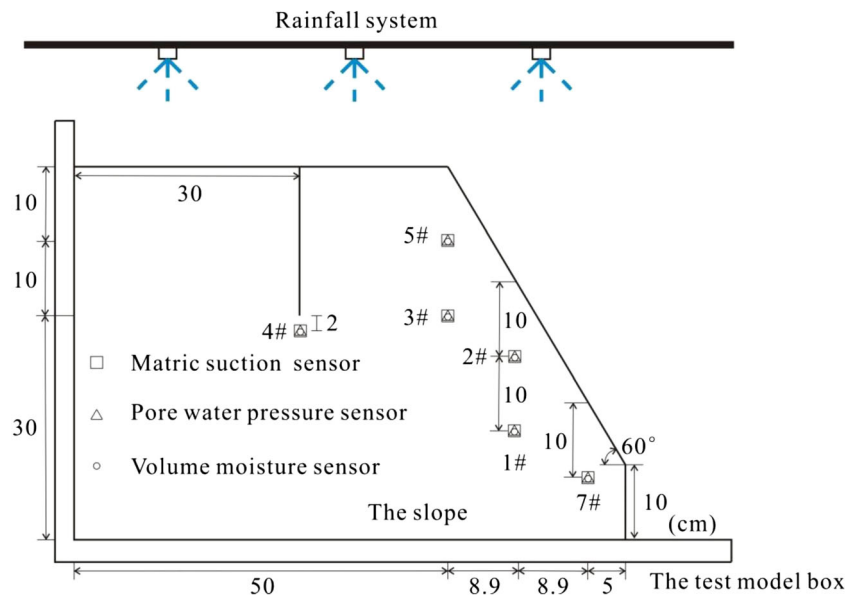**Fig. 7** The prototype slope and the model slope

(a) The prototype slope

(b) The model slope

Fig. 8 Experimental section of slope containing a vertical joint with continuous heavy rainfall

At 5 h and 20 min, the pore-water pressure suddenly increases, which is a main factor inducing the slope sliding. The increment of sensor 2 is largest because the position of soil particle changed due to shearing. The pore-water pressure near the sliding surface suddenly increases, which creates the excess pore-water pressure. The sliding distance of point 2 located at the landslide front is largest, and the shearing speed is the largest. Therefore, the excess pore-water pressure is also relatively high. The change in pore-water pressure is not consistent with the water content, because the pore-water pressure sensor and the moisture content sensor are at different positions.

Loess slope containing a vertical joint with continuous heavy rainfall

As shown in Fig. 13, we can see the process of deformation and failure of loess slope containing a vertical joint with continuous heavy rainfall. The sequence of seepage velocity from large to small was: the joint, toe of slope, trailing edge of the slope, and middle slope. From Figs. 14, 15, and 16, among all the sensors, readings of volume moisture sensor 4 located 2 cm below the joint increased gradually before rising sharply when landslide occurred. Among the sensors 2, 5, and 7 buried at 10 cm depths, readings of sensor 7 buried at the trailing edge of the slope increased earlier than that of the remaining two sensors, and did not change significantly with the occurrence of landslide. Then sensor 5 located below the shoulder of the slope increased slightly when a sliding failure was formed. Reading of sensor 2 buried at the middle slope changed last, and increased obviously when slope sliding happened. Among the sensors 1 and 3 buried at

20 cm depths, reading of sensor 1 buried at the middle slope changed initially and then rose slightly when the slope failure occurred. Then followed sensor 3 located below the shoulder of slope, and the trend of change was the same as that of sensor 1. The order of the decreasing readings of matric suction sensors was in the same order as that of the volumetric water content sensors, and the difference was the same as that of the loess slope with continuous heavy rainfall experiment. The trend of the increasing readings of pore-water pressure sensors coincide with the trend of changing readings of volumetric water content sensors. During the sliding of the slope, when volumetric water content rose sharply, it was accompanied by a sudden increase in pore-water pressure. Moreover, the biggest increasing range of readings among all pore-water pressure sensors was sensor 1 located 20 cm below the middle slope.

As for the volumetric water content of sensors, sensor 5 is located below the shoulder, the rainwater on the trailing edge flows through the shoulder, causing erosion. Sensor 2 is located below the slope, and water runoff is easy. Therefore, compared with sensor 2, sensor 5 began to increase earlier. After 3 h and 24 min, the loess became basically saturated, and the water content remained basically unchanged. The moisture content of sensor 2 began to obviously increase. The readings of sensor 2 and sensor 5 suddenly increased at 4 h and 32 min, when the loess slope slid.

The change in pore-water pressure sensors was consistent with volumetric moisture sensors. Sensor 5 started to increase earlier than sensor 2, and then the pore-water pressure increased significantly. The pore-water pressure suddenly changed at 4 h and 32 min, and then the pore-water pressure gradually dissipated, which led to the landslide.

Fig. 9 Experimental process of loess slope with continuous heavy rainfall

(a) The initial state

(b) Erosion of water at the slope shoulder and toe

(c) Partial failure of the slope

(d) Integral failure of the slope
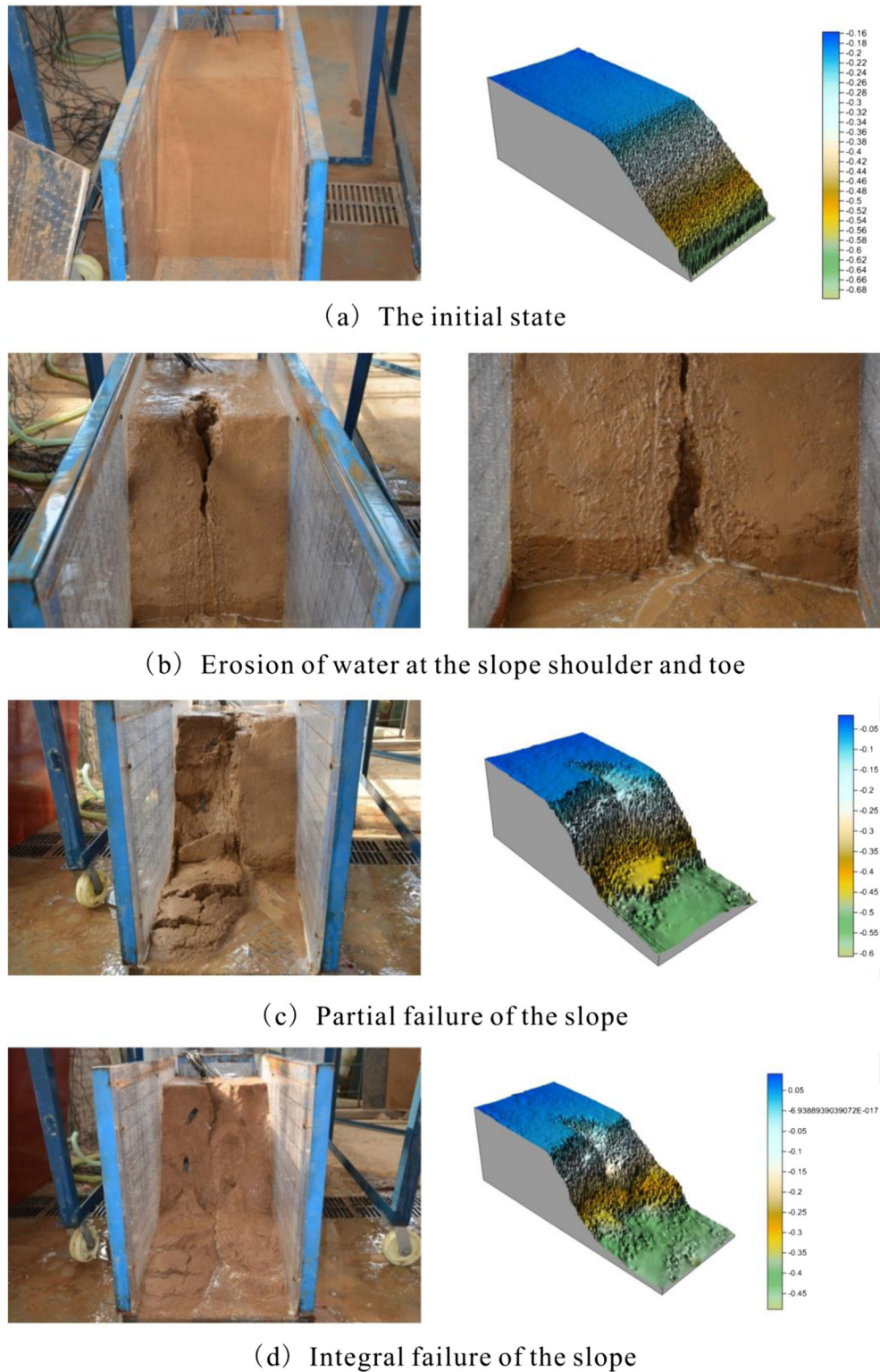
Loess slope with intermittent heavy rainfall

The process of deformation and failure of loess slope with intermittent heavy rainfall is the same with that of loess slope with continuous heavy rainfall; as a result, the authors will not reiterate them here. From Figs. 17, 18, and 19, the authors found the seepage velocity from large to small was the same order as that of the loess slope with continuous heavy rainfall. Among the sensors 2, 5, 6, and 7 buried at 10 cm depths, readings of sensor 7 buried at
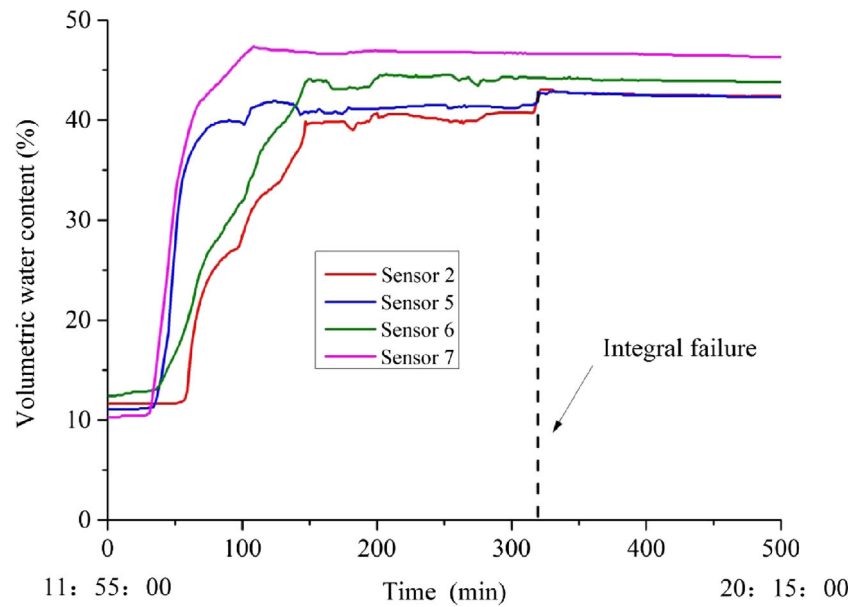
(a) Changes in volumetric water content of sensors 2, 5, 6 and 7
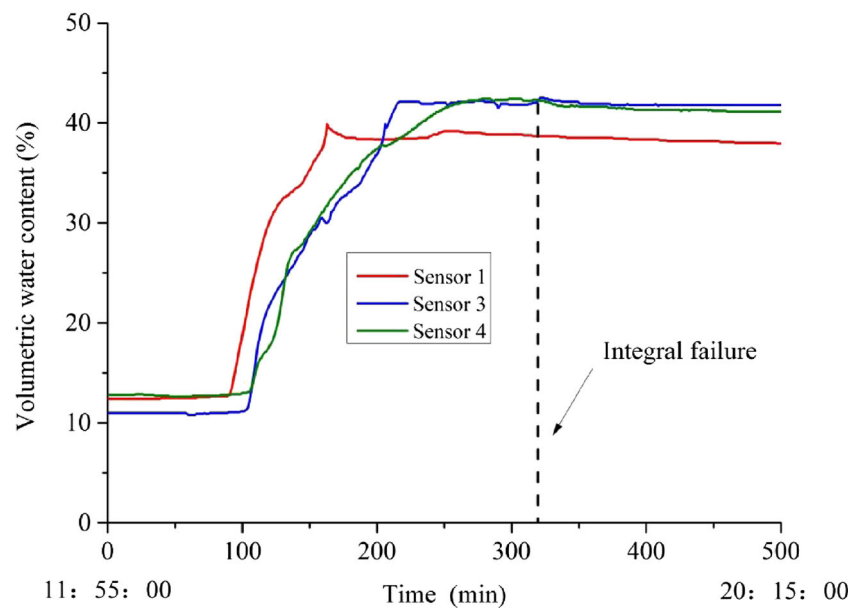
(b) Changes in volumetric water content of sensors 1, 3 and 4

the foot of the slope rose initially, and decreased after the cessation of rain and increased again after the beginning of rainfall, but the increasing range decreased gradually. There was no obvious increasing range in readings when sliding failure was initiated. The order of increasing readings of other sensors was the same with that of loess slope with continuous heavy rainfall, and these sensors had the same changing readings trend as sensor 7. However, only readings of sensor 2 located at 10 cm below the middle slope and sensor 5 buried at 10 cm depths below the slope shoulder showed a sudden rise of the sensor when the

slope failure happened. The order of the decreasing readings of matric suction sensors was consistent with that of the volumetric moisture sensors, and the difference is when the readings of matric suction sensors reached a certain value and increased slightly after the cessation of rain and decreased after the beginning of rainfall, but the rate of decrease waned gradually. The trend of the increasing readings of pore-water pressure sensors coincide with the trend of changing readings of volumetric water content sensors. When volumetric water content rose, it was accompanied by an increase in pore-water pressure, and

Fig. 11 Reading changes in matric suction sensors of the loess slope with continuous heavy rainfall
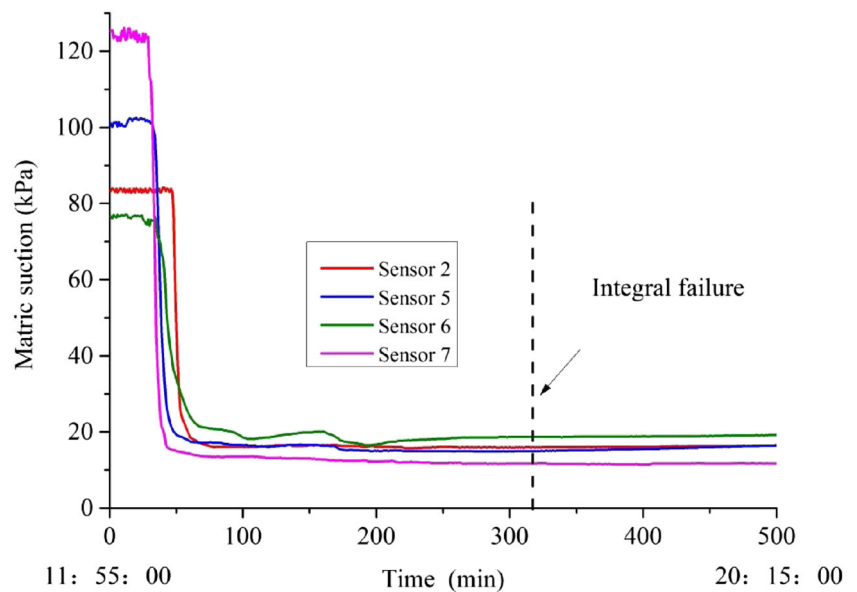
(a) Changes in matric suction of sensors 2, 5, 6 and 7
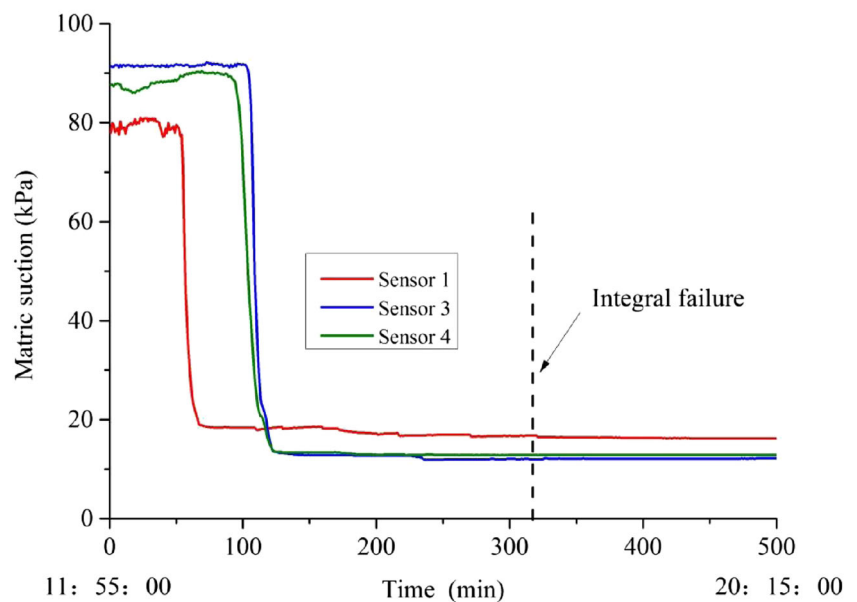

(b) Changes in matric suction of sensors 1, 3 and 4

showed dissipation of pore-water pressure after the cessation of rain. The biggest increasing range of readings among all pore-water pressure sensors is sensor 2 located 10 cm below the middle slope.

Volumetric water content sensor 5 is located under the shoulder of the slope, the water content starts to increase earlier, and increases significantly at 57 min. The rain continued the next 5 days with the same rainfall intensity. The difference between the maximum and minimum values of sensor reading

became smaller and smaller as the loess slope became gradually saturated. On the sixth day, water content increased to 44.6% and remained basically stable. When water content suddenly increased the landslide occurred.

Pore-water pressure sensor, sensor 5 began to increase at 36 min, and gradually decreased after reaching the peak value of 0.3 kPa. The change trend of pore-water pressure in the second, third, fourth, and fifth days was consistent with the change trend of volumetric moisture

Fig. 12 Reading changes in pore water pressure sensors of the loess slope with continuous heavy rainfall
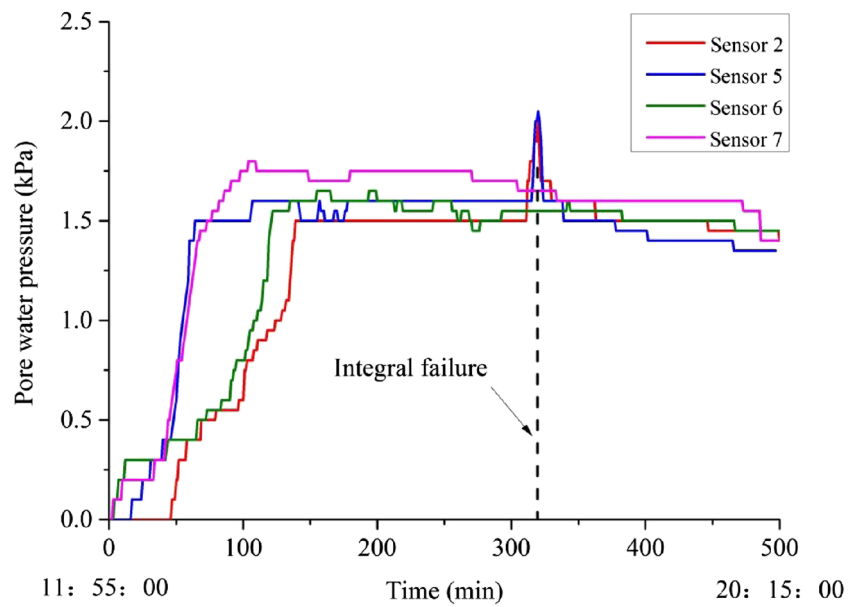
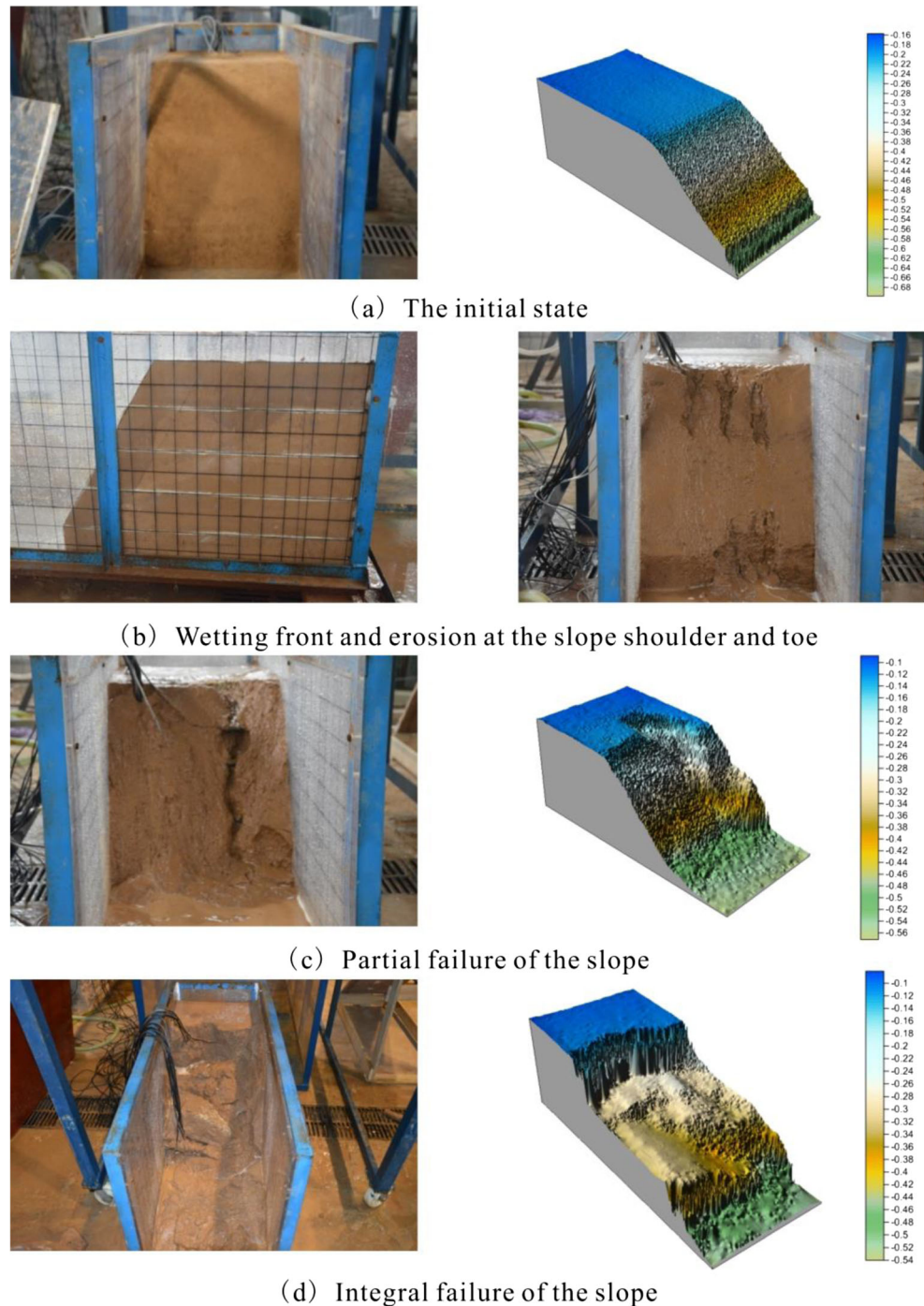(a) Changes in pore water pressure of sensors 2, 5, 6 and 7
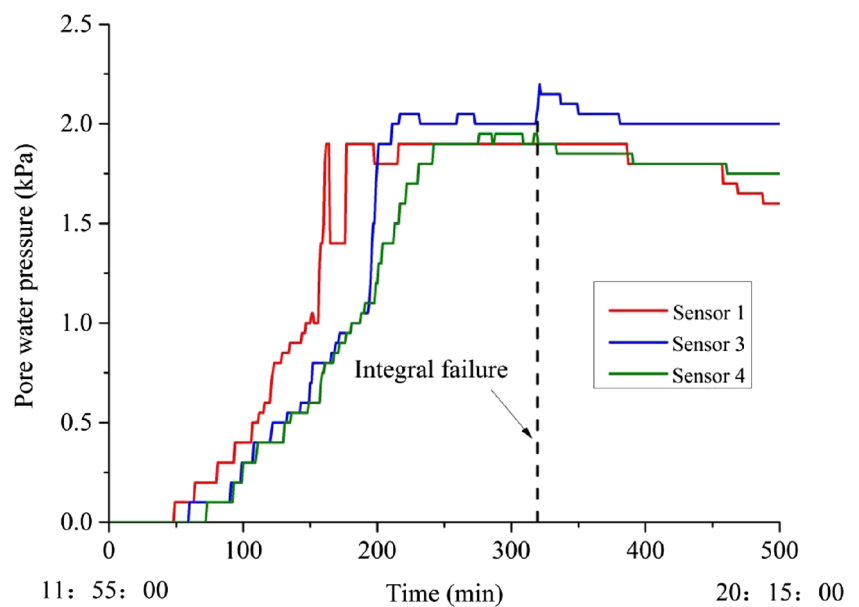
(b) Changes in pore water pressure of sensors 1, 3 and 4

content of sensor 5. On the sixth day, the pore-water pressure increased slightly, while the slope slid as a whole. Reading of sensor 2 began to increase after 57 min and reached 0.5 kPa. The change trend of pore-water pressure in the next 5 days was consistent with that in water content. Pore-water pressure suddenly increased, which is a main indicator of the loess slope sliding.

In summary, under the condition of rainfall, the sudden rise in volumetric water content and the accompanying sudden increase in pore-water pressure is the main factor inducing the landslide. It was found that the smaller the distance between pore-water pressure sensor and sliding surface, the greater the increasing range of the readings. During the same period, there were no obvious changes in the readings of matric suction sensors when the landslide occurred, which indicated that there was no significant correlation between the change of matric suction and the occurrence of landslide, which can be seen in Table 3.

Fig. 13 Experimental process of the loess slope containing a vertical joint with continuous heavy rainfall

(a) The initial state

(b) Wetting front and erosion at the slope shoulder and toe

(c) Partial failure of the slope

(d) Integral failure of the slope

Failure mode and triggering mechanism for landslide

### Failure mode of loess slope with continuous heavy rainfall

The failure mode of loess slope with continuous heavy rainfall is shown in Fig. 20. Four stages are stated as follows:

(1) Erosion at the slope shoulder: Rainwater concentrated on the trailing edge of the slope flowed along the slope surface, eroding the slope shoulder and erosion gradually decreased from top to bottom.

(2) Erosion at the slope toe: After the first stage, rainwater was concentrated at the slope bottom and softened the slope toe as the intensity of erosion reduced gradually from bottom to top, all of which aided the formation of a free surface at the slope toe.

Fig. 14 Reading changes in volumetric moisture sensors of the loess slope with a vertical joint
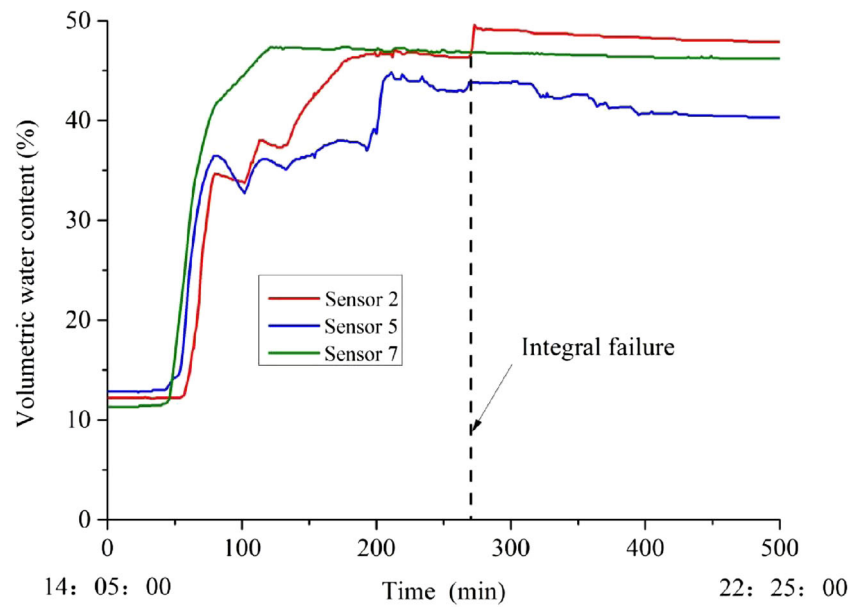
(a) Changes in volumetric water content of sensors 2, 5 and 7
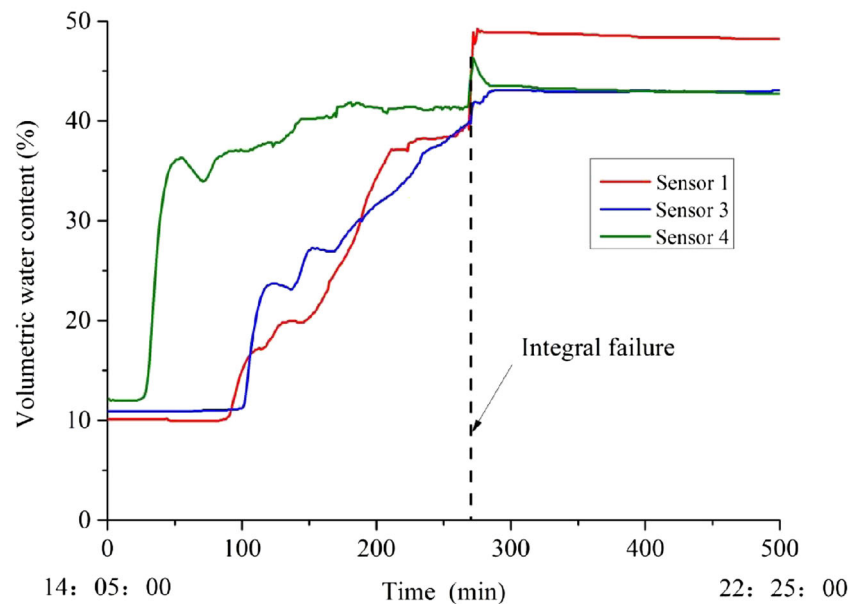
(b) Changes in volumetric water content of sensors 1, 3 and 4

(3) Formation and growth of crack in the trailing edge of the slope: Upper loess had a tendency to move down along the slope surface under the influence of gravity. With increasing water content, the strength of the loess slope decreased. Finally, cracks were formed and extended gradually in the trailing edge of the slope.

(4) Integral failure of the slope with steep sliding plane: With partial failures extended constantly, pore-water pressure was generated when the rainwater entered the cracks. The high saturation of the loess and the accompanying reduction in strength resulted in the gradual generation of

a steep sliding surface. Landslide did not occur until the pore-water pressure reached a certain value and cracks were intersected.
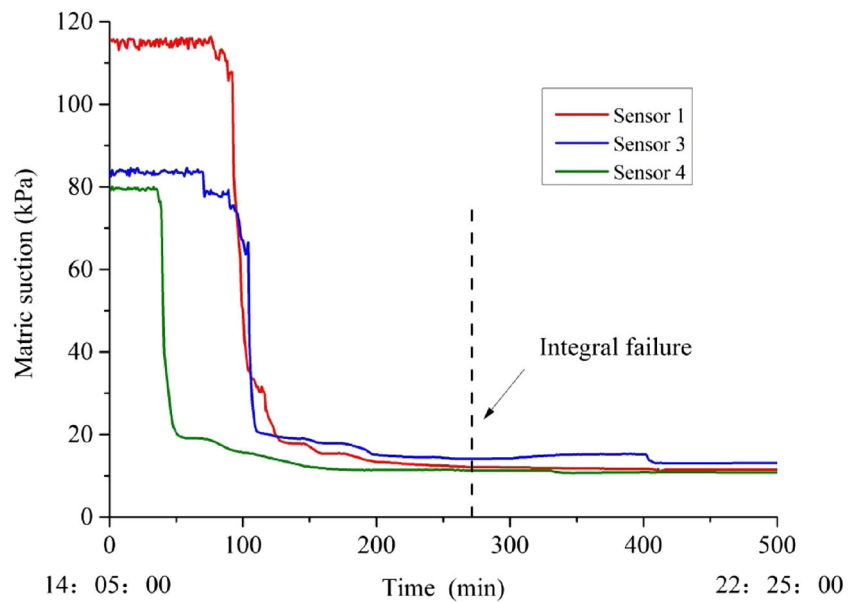
Failure mode of loess slope containing a vertical joint with heavy rainfall

As shown in Fig. 21, it can be seen that the failure mode of loess slope containing a vertical joint with continuous heavy

Fig. 15 Reading changes in
matric suction sensors of the loess
slope with a vertical joint
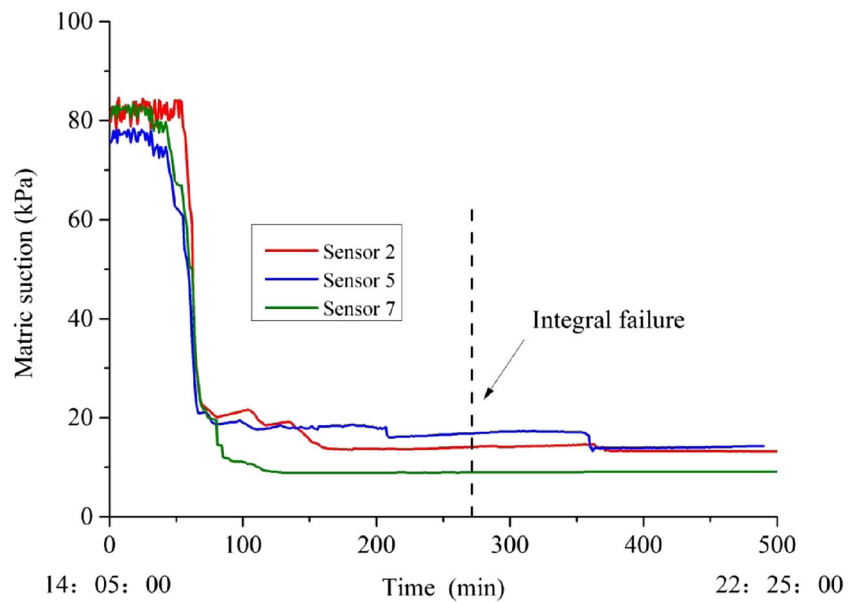


(a) Changes in matric suction of sensors 2, 5 and 7


(b) Changes in matric suction of sensors 1, 3 and 4

rainfall is quite different from that of loess slope with continuous heavy rainfall, and more details about the failure mode are as follows:

(1) Stage of erosion at the slope shoulder: Rainwater concentrated on the trailing edge of the slope flowed along with the slope surface and eroded the shoulder of the slope. The intensity of erosion decreased gradually from top to bottom.

(2) Stage of erosion at the toe of the slope: After the last stage, rainwater was concentrated at the slope bottom

and softened the slope toe, and the intensity of erosion reduced gradually from bottom to top.

(3) Stage of vertical growth of joint: The joint was filled with rainwater, and pore-water pressure was generated. With the strength of loess reduced, the joint was mostly extended in a vertical direction, and a gentle sliding plane gradually developed.

(4) Stage of deep-seated landslide: The deep-seated landslide occurred due to vertical crack and gentle sliding plane.

Fig. 16 Reading changes in pore water pressure sensors of the loess slope with a vertical joint
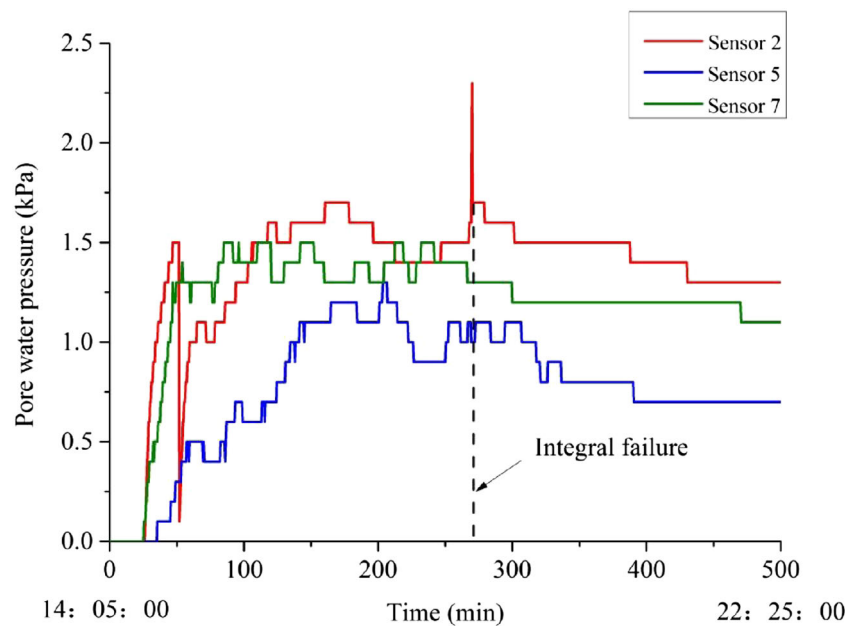
(a) Changes in pore water pressure of sensors 2, 5 and 7
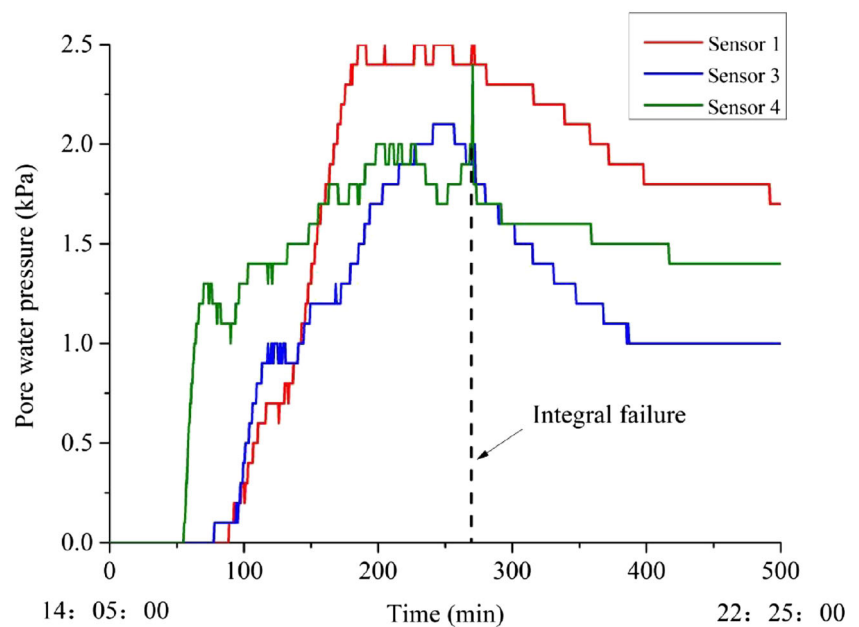
(b) Changes in pore water pressure of sensors 1, 3 and 4

Failure mode of loess slope with intermittent heavy rainfall

Failure mode of loess slope with intermittent heavy rainfall is the same as that of loess slope with continuous heavy rainfall, while in the third stage, heterogeneity of extension and shrinkage in loess and gravity of upper loess upon free surface located at slope bottom are the two factors for the formation of cracks in the trailing edge of the slope. The rest is identical to the mode of loess slope with continuous heavy rainfall.

For homogeneous slopes (continuous heavy rainfall slope experiment and intermittent heavy rainfall slope experiment), the soil is unsaturated in the early stage of rainfall. As the rainfall continues, the volumetric water content continues increasing and the shear strength decreases accordingly. In the

Fig. 17 Reading changes in volume moisture sensors of the loess slope with a intermittent heavy rainfall
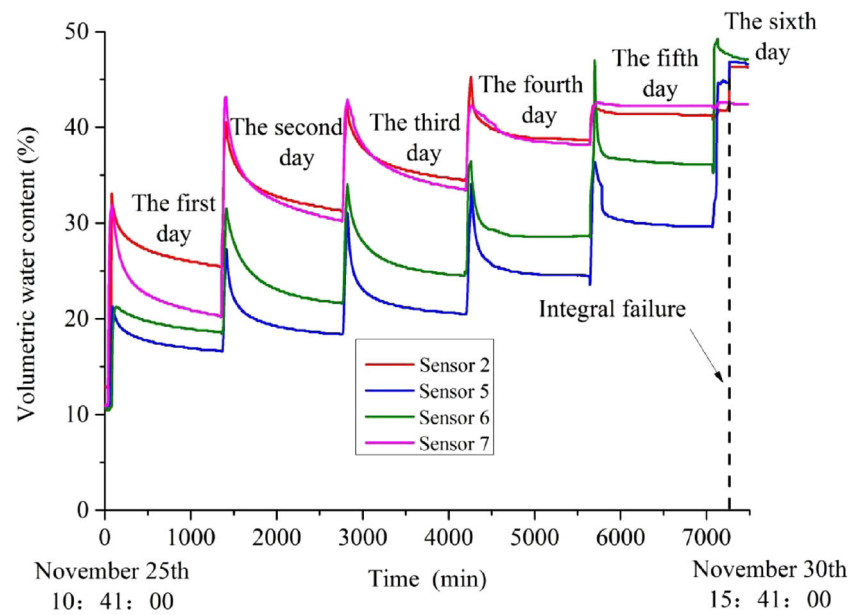
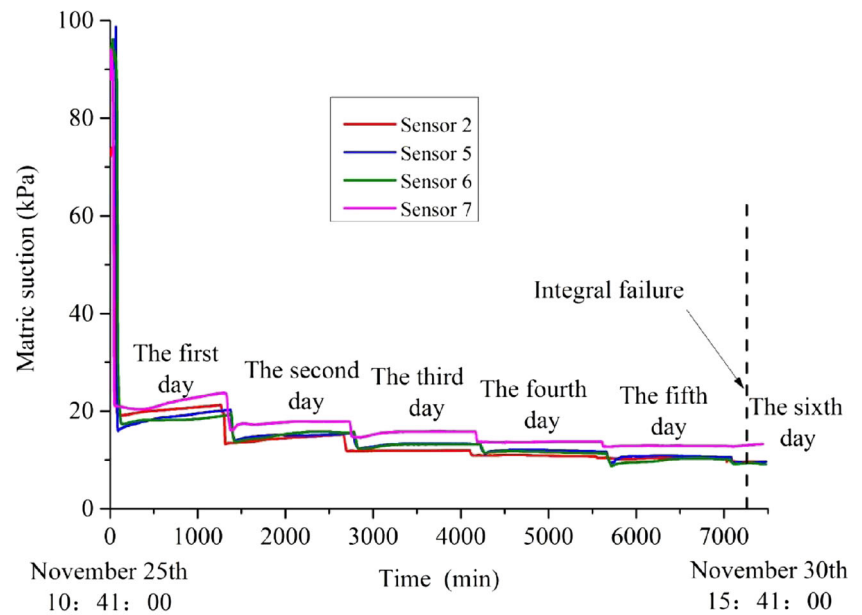(a) Changes in volumetric water content of sensors 2, 5, 6 and 7
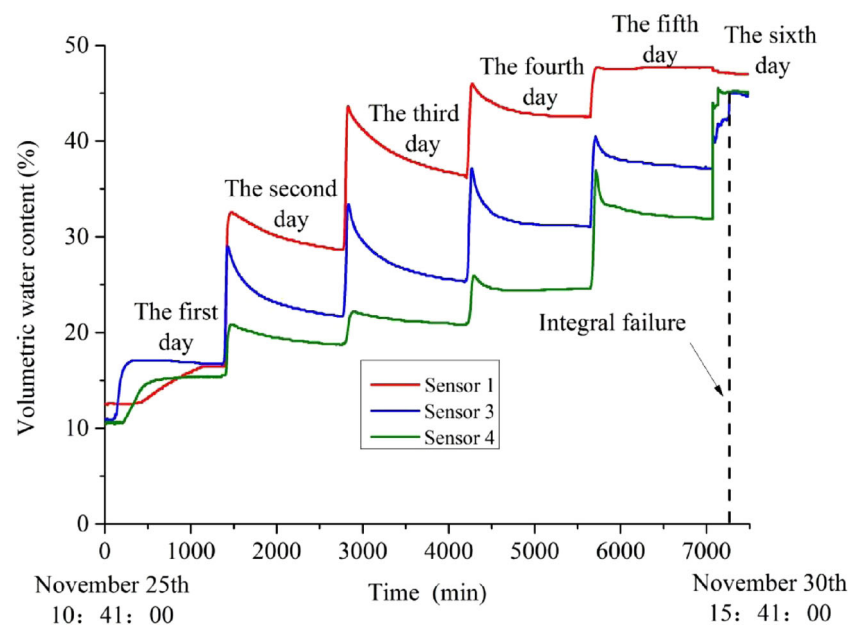
(b) Changes in volumetric water content of sensors 1, 3 and 4

later stage of the experiment, the upper soil becomes saturated, and the pore-water pressure is basically steady. As the trailing edge cracks are generated, water enters the fissure and further promotes the expansion of the fissure, resulting in continuous deformation of the slope. The effective stress of the loess slope is reduced due to increasing excess pore-water pressure. When it is reduced to a critical value, the cracks extend to form the main slip surface, and the landslide occurs. The loess slope with vertical joints is unsaturated in the early stage of rainfall.

As the rainfall continues, the superficial layer becomes gradually saturated, and the rainwater accumulates at the trailing edge of the slope, where water is filled inside the joint.

Meanwhile, due to the slope foot erosion, the slope becomes steep. The loess softening at the slope foot makes shearing strength decrease. Expansion of joints and generation of new cracks result in continuous deformation of the loess slopes. During the deformation process, some part of the soil is not well drained, and excess pore-water pressure is

Fig. 18 Reading changes in matric suction sensors of the loess slope with a intermittent heavy rainfall

(a) Changes in matric suction of sensors 2, 5, 6 and 7
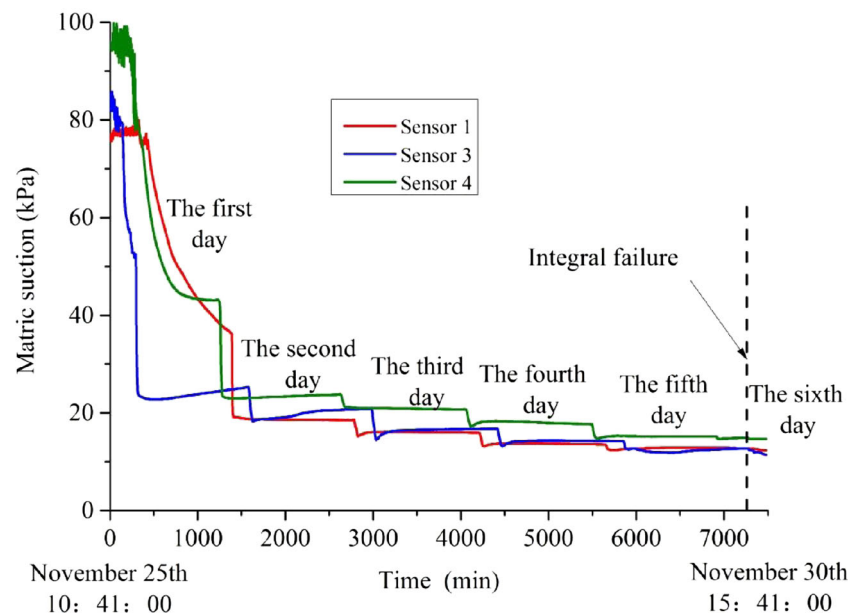
(b) Changes in matric suction of sensors 1, 3 and 4

generated, and the effective stress is reduced. When the soil strength is reduced to the critical value, a slip surface is formed along the joints and the generated cracks, and the slide occurs.

Conclusions

Based on the experimental results, we draw the following conclusions:

(1) In the early stage of the experiments, the matric suction of the loess decreased gradually and remained stable in the end; therefore, the strength reduced, with the continuous increases of volumetric water content. In the later stage the upper loess of the slope became saturated, excess pore-water pressure generated by the slope deformation and weak drainage of the loess decreased the effective stress and the loess strength, which resulted in landslides. Meanwhile, the increase range of volumetric water content in

Fig. 19 Reading changes in pore water pressure sensors of the loess slope with a intermittent heavy rainfall
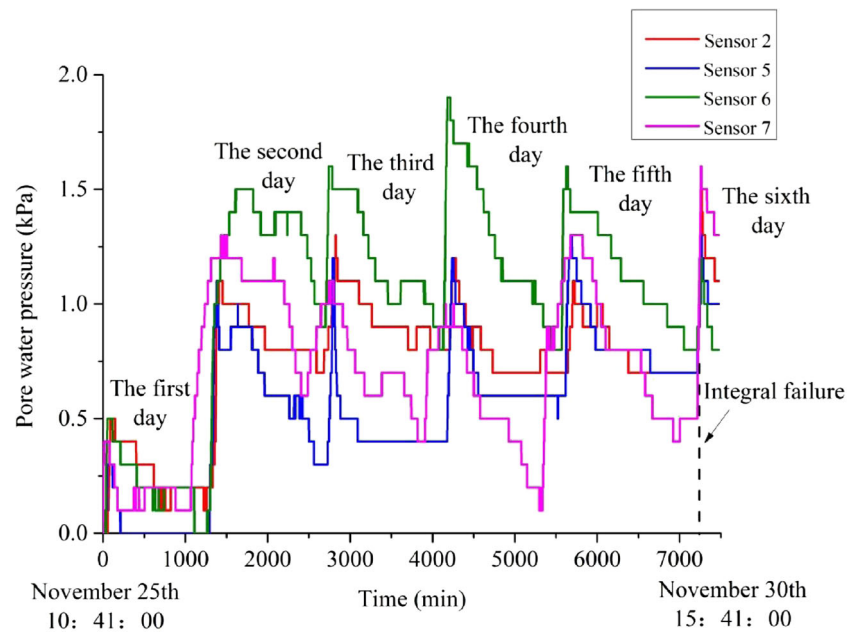
(a) Changes in pore-water pressure of sensors 2, 5, 6 and 7
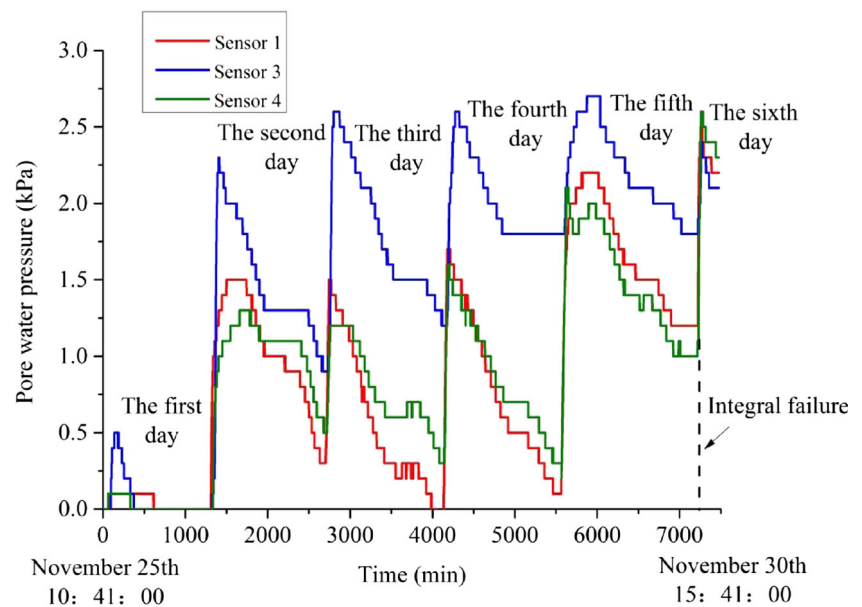
(b) Changes in pore-water pressure of sensors 1, 3 and 4

loess slopes with continuous heavy rainfall experiment was very great when sliding occurred.

(2) Continuous heavy rainfall easily produces marked deformation of loess slopes, particularly those containing a vertical joint. The influence of slope structure on slope stability is greater than that of rainfall patterns. The time needed in loess slope containing a vertical joint with continuous heavy rainfall experiment was the shortest, while the time needed in loess slope failure with intermittent heavy rainfall experiment was the longest. It is

concluded that the vertical joint affects the integrity of the slope and accelerates its deformation during rainfall, which was conducive to the occurrence of landslide.

(3) Under the condition of no preformed joint in loess slope, the deeper the sliding surface is, the larger the pore-water pressure needed in the slope. In addition, the deeper the sliding surface is, the longer the time needed for the landslide failure.

(4) The failure mode of loess slope with continuous heavy rainfall consists of four stages: a) The original slope; b)

Table 3 Development and sliding time of rainfall-induced landslides

| Experimental type	Deformation and failure	Cumulative precipitation(mm)	Sliding time (min)
Loess slope with continuous heavy rainfall	① Erosion occurs at the slope shoulder and toe. ② Slight settlement was shown in the trailing edge of the slope and cracks occurred 5 cm away from the shoulder. ③Sliding velocity was relatively high, sliding distance was short, and sliding surface was shallow.	373.3	320
Loess slope containing a vertical joint with continuous heavy rainfall	① Erosion on the slope shoulder and toe was strong. ② Joint was filled with rainwater and slight collapse occurred, then it expanded downward, and wetting front showed an arc. ③ Sliding velocity was high, and sliding surface was very deep.	318.5	273
Loess slope with intermittent heavy rainfall	① Erosion at the slope shoulder can be seen, and collapse occurred at the slope toe. ② After one-day rainfall, many tiny cracks were generated in the trailing edge of the slope, which were 9 cm away from the shoulder; and were filled with rainwater when rained. ③ Sliding time was very long, and sliding distance was the shortest.	415.3	7263 (5 days 1 h 3 min)
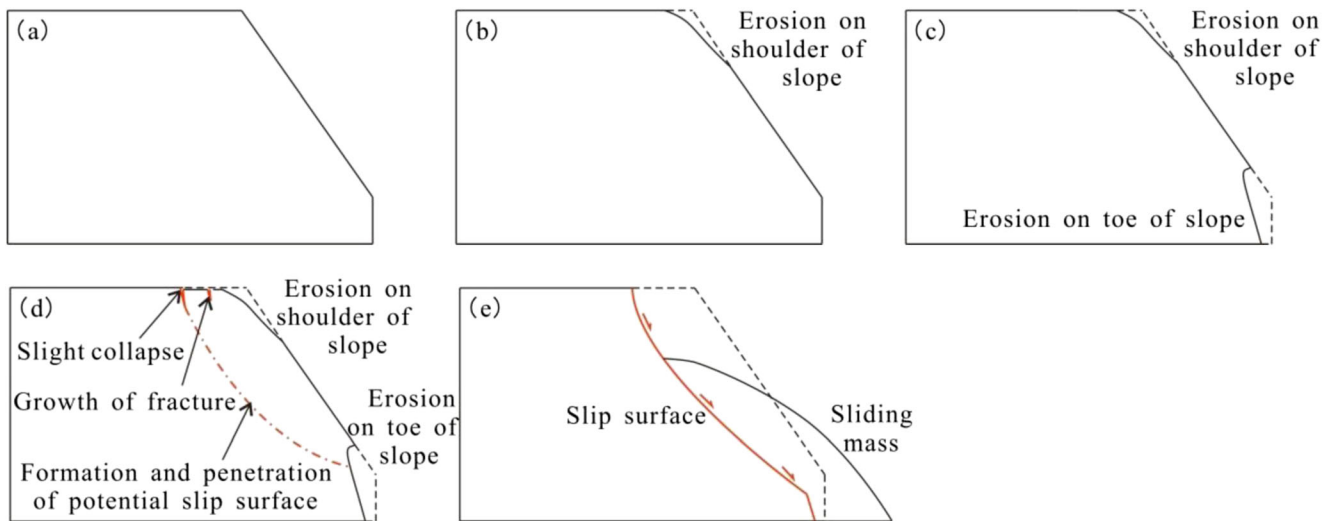
Fig. 20 Failure mode of landslides induced by continuous heavy rainfall
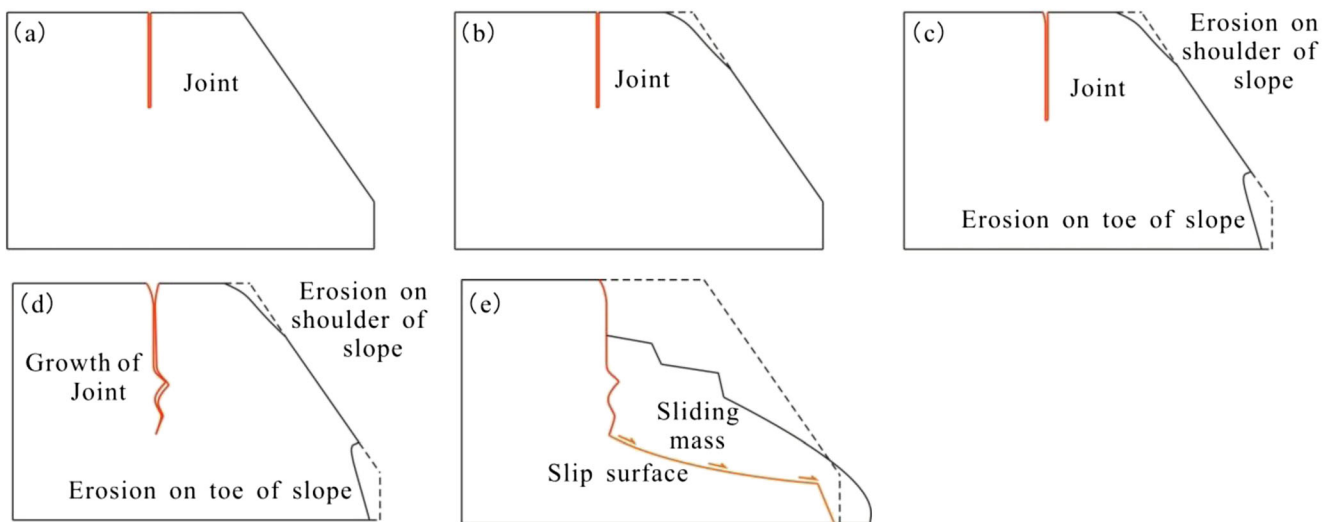

Fig. 21 Failure mode of landslides (contained vertical joint) induced by continuous heavy rainfall

Erosion of water at the slope shoulder; c) Erosion of water at the toe of the slope; d) Formation and growth of fracture in the trailing edge of the slope; e) Sliding failure of the slope; while failure mode of loess slopes containing a vertical joint with continuous heavy rainfall is quite different because the joint in the trailing edge of the slope develops in a vertical direction with deep-seated sliding.

References

Aleotti P (2004) A warning system for rainfall-induced shallow failures. Eng Geol 73:247–265

Ali A, Huang J, Lyamin A, Sloan S, Cassidy M (2014) Boundary effects of rainfall-induced landslides. Comput Geotech 61:341–354

Anderson SA, Sitar N (1995) Analysis of rainfall-induced debris flow. J Geotech Eng 121:545–552

Chang K, Chiang S (2009) An integrated model for predicting rainfall-induced landslides. Geomorphology 105:366–373

Chen H, Lee C (2003) A dynamic model for rainfall-induced landslides on natural slopes. Geomorphology 51:269–288

Claessens L, Schoorl JM, Veldkamp A (2007) Modelling the location of shallow landslides and their effects on landscape dynamics in large watersheds: an application for northern New Zealand. Geomorphology 87:16–27

Collins B, Znidarcic D (2004) Stability analyses of rainfall induced landslides. J Geotechn Geoenviron Eng 130(4):362–372

Crozier MJ (1999) Prediction of rainfall-triggered landslides: a test of the antecedent water status model. Earth Surf Proc Land 24:825–833

Evans SG, Roberts NJ, Ischuk A, Delaney KB, Morozova GS, Tutubalina O (2009) Landslides triggered by the 1949 Khait earthquake, Tajikistan. and associated loss of life Eng Geol 109(3-4):195–212

Gao GR (1988) Formation and development of the structure of collapsing loess in China. Eng Geol 25:235–245

Godt JW, Baum RL, Chleborad AF (2006) Rainfall characteristics for shallow landsliding in Seattle, Washington. USA Earth Surf Proc Land 31:97–110

Guzzetti F, Cardinali M, Reichenbach P, Cipolla F, Sebastiani C, Galli M, Salvati P (2004) Landslides triggered by the 23 November 2000 rainfall event in the Imperia Province, Western Liguria. Italy Eng Geol 73:229–245

Hovius N, Stark CP, Allen PA (1997) Sediment flux from a mountain belt derived by landslide mapping. Geology 25:231–234

Liu D (1985) Loess and environment. Science Press, Beijing, pp 1–43 (in Chinese)

Peng JB, Fan ZJ, Wu D, Zhuang JQ, Dai FC, Chen WW, Zhao C (2015) Heavy rainfall triggered loess–mudstone landslide and subsequent debris flow in Tianshui. China. Eng. Geol. 186:79–90

Peng JB, Sun P, Igwe O, Li XA (2017) Loess caves, a special kind of geo-hazard on loess plateau, northwestern China. Eng Geol. https://doi.org/10.1016/j.enggeo.2017.08.012

Rosenau M, Lohrmann J, Oncken O (2009) Shocks in a box: an analogue model of subduction earthquake cycles with application to seismotectonic forearc evolution. J Geophys Res Solid Earth 114: B01409

Tsai T (2011) Influences of soil water characteristic curve on rainfall-induced shallow landslides. Environ Earth Sci 64(2):449–459

Tsaparas I, Rahardjo H, Toll D, Leong E (2002) Controlling parameters for rainfall induced landslides. Comput Geotech 29(1):1–27

Tu XB, Kwong AKL, Dai FC, Tham LG, Min H (2009) Field monitoring of rainfall infiltration in a loess slope and analysis of failure mechanism of rainfall-induced landslides. Eng Geol 105:134–150

Wang GH, Zhang DX, Furuya G, Yang J (2014) Pore-pressure generation and fluidization in a loess landslide triggered by the 1920 Haiyuan earthquake, China: a case study. Eng Geol 174:36–45

Wu LZ, Zhou Y, Sun P, Shi JS, Liu GG, Bai LY (2017) Laboratory characterization of rainfall-induced loess slope failure. Catena 150: 1–8

Wu LZ, Deng H, Huang RQ, Zhang LM, Guo XG, Zhou Y (2018a) Evolution of lakes created by landslide dams and the role of dam erosion: A case study of the Jiajun landslide on the Dadu River, China. Quatern Int. https://doi.org/10.1016/j.quaint.2018.08.001

Wu LZ, Zhang LM, Zhou Y, Xu Q, Liu GG, Bai LY (2018b) Theoretical analysis and model test for rainfall induced shallow landslides in the red-bed area of Sichuan. Bull Eng Geol Environ 77(4):1343–1353

Xu L, Dai FC, Tham LG, Tu XB, Min H, Zhou YF, Wu CX, Xu K (2011) Field testing of irrigation effects on the stability of a cliff edge in loess, north-West China. Eng Geol 120:10–17

Xu L, Dai FC, Gong QM, Tham LG, Min H (2012) Irrigation-induced loess flow failure in Heifangtai platform. North-West China Environ Earth Sci 66:1707–1713

Zhang J, Jiao JJ, Yang J (2000) In situ rainfall infiltration studies at a hillside in Hubei province. China Eng Geol 57:31–38